

DEVELOPMENT AND EVALUATION OF BOSWELLIA-LOADED SOLID LIPID NANOPARTICLE FILMS FOR TRANSDERMAL DELIVERY IN CARRAGEENAN-INDUCED ARTHRITIS MODEL IN RATS

SONIA K.¹, R. VIJAYA², V. JANANI³, KIRUBA MOHANDOSS^{4*}

¹Department of Pharmaceutical Chemistry, Sri Ramachandra Faculty of Pharmacy, Sri Ramachandra Institute of Higher Education and Research (DU), Porur, Chennai-116, India. ^{2,3}Department of Pharmaceutical Technology, University College of Engineering, Anna University, BIT Campus, Tiruchirapalli, India. ⁴Department of Pharmaceutics, Sri Ramachandra Faculty of Pharmacy, Sri Ramachandra Institute of Higher Education and Research (DU), Porur, Chennai-116, India

*Corresponding author: Kiruba Mohandoss; *Email: mkirupa@sriramachandra.edu.in

Received: 24 May 2025, Revised and Accepted: 22 Sep 2025

ABSTRACT

Objective: This study aimed to develop and evaluate a dual-purpose solid lipid nanoparticle (SLN)-chitosan/PVA matrix-based transdermal film incorporating *Boswellia serrata* extract for enhanced anti-arthritic activity, sustained drug release, and improved biocompatibility.

Methods: Boswellia-loaded SLNs were prepared using hot homogenization at 15,000 rpm for 15 min with stearic acid as lipid and Polysorbate 80 as surfactant. The optimized nanoparticles (lipid-to-drug ratio 8:1) were embedded in a chitosan-polyvinyl alcohol (PVA) film-forming matrix. Three formulations (F1-F3) were developed and evaluated for physicochemical properties, drug content uniformity, and swelling index. Advanced techniques, including SEM, FTIR, and zeta analysis, were used for characterization. *In vitro* drug release was studied via the Franz diffusion cell using a cellulose acetate membrane (pH 7.4), and kinetics were modelled. Antioxidant activity was assessed via DPPH and nitric oxide assays, while anti-inflammatory effects were studied through protease, lipoxygenase, and protein-denaturation assays. Biocompatibility was tested using RAW 264.7 macrophages (MTT assay). *In vivo* studies included Draize-based skin irritation and carrageenan-induced paw edema models in wistar rats.

Results: The F2 formulation exhibited optimal characteristics with a surface pH of 6.4, drug content uniformity of 98.3%, and a swelling index of 152.8%. Particle size distribution (PDI 0.410) and zeta potential (-29.9 mV) confirmed stability. SEM showed spherical particles with smooth surfaces. FTIR revealed characteristic drug-polymer interactions. *In vitro* drug release followed a biphasic pattern with an initial burst and sustained diffusion, achieving 98.38% release over 6 h. Antioxidant assays showed 89.6% DPPH and 85.9% nitric oxide inhibition. The film significantly inhibited inflammatory enzymes, with results comparable to diclofenac sodium. Cell viability remained >80% even at 200 µg/ml. No signs of dermal irritation were noted. *In vivo*, the film reduced paw edema by over 50% at 8 h.

Conclusion: The HSLN-loaded chitosan/PVA film demonstrated biphasic drug release, potent anti-inflammatory and antioxidant activity, and excellent biocompatibility, making it a promising non-invasive therapeutic strategy for managing arthritis. The biphasic release profile offers rapid symptom relief followed by sustained action, which may reduce dosing frequency and improve patient compliance in chronic RA therapy. Further clinical investigations are warranted.

Keywords: Boswellic acid, Solid lipid nanoparticles, Transdermal film, Anti-arthritic, Good health well-being, Industry innovation and infrastructure

© 2025 The Authors. Published by Innovare Academic Sciences Pvt Ltd. This is an open access article under the CC BY license (<https://creativecommons.org/licenses/by/4.0/>) DOI: <https://dx.doi.org/10.22159/ijap.2025v17i6.55187> Journal homepage: <https://innovareacademics.in/journals/index.php/ijap>

INTRODUCTION

Synovial joints are the primary target of rheumatoid arthritis (RA), a chronic, systemic inflammatory disease that causes inflammation, discomfort, stiffness and eventual joint destruction. It is one of the most crippling musculoskeletal conditions, affecting almost 1% of the world's population, particularly middle-aged and older people. Recent data from the Global Burden of Disease (GBD) study 2020 and 2017 reported over 17 million individuals living with RA globally, with an increasing trend in age-standardized prevalence (208.8 per 100,000) and incidence (13.48 per 100,000 adults aged 20-56), emphasizing its growing global impact [1]. The weight of disease permeates the socioeconomic and emotional sphere, thereby lowering the quality of life and raising medical expenses [2]. Clinical radiographic and serological evaluations have historically been used in conjunction for the diagnosis and treatment of RA in order to ascertain disease activity and direct treatment. In order to reduce inflammation and stop permanent joint damage, current therapeutic approaches place a strong emphasis on early and intensive pharmaceutical intervention. However, systemic adverse effects. Toxicity and problems are frequently linked to long-term use of these drugs [3].

Scientific interest has recently shifted to plant-based remedies like Indian frankincense or *Boswellia serrata*, which has been thoroughly investigated for its anti-arthritic properties. Boswellic acids, which are found in the gum resin of *Boswellia serrata*, prevent the

formation of leukotrienes by inhibiting the enzyme 5-lipoxygenase. With a relatively safer profile than traditional NSAIDs, Boswellia-based formulations have been shown in numerous preclinical and clinical studies to reduce morning stiffness, increase mobility and reduce joint edema in patients with RA.

Herbal treatments have limited clinical value due to a number of formulation issues, notwithstanding their medicinal promise. Because of their substantial first-pass metabolism, many phytoconstituents are lipophilic, weakly soluble, and have lower oral bioavailability [4]. The use of nanotechnology in the delivery of herbal medications is one novel approach to address these issues. A potent tactic for enhancing the solubility, stability and targeted administration of herbal substances is nano-phytomedicine. When designed for transdermal applications, Herbal solid lipid nanoparticles (HSLNs) provide a flexible platform for encapsulating lipophilic plant-based actives, such as boswellic acids, allowing for increased skin penetration, regulated drug release and protection against degradation.

Using Herbal solid lipid nanoparticles (HSLNs) in a biopolymeric chitosan-polyvinyl alcohol (PVA) matrix, the study offers a dual-purpose transdermal delivery system in the treatment of RA. In particular, this technique presents a potential approach for the prolonged and improved delivery of herbal actives. This creates a functionally strong and therapeutically superior film by fusing nanoencapsulation with the bioadhesive, film-forming and

biocompatible qualities of PVA and chitosan polymers. HSLNs help with regulated drug release, stabilize bioactive molecules, and increase solubility. The chitosan-PVA matrix promotes medication retention at the application site by forming a protective barrier and assisting in the uniform dispersion of HSLNs. Recent studies by Khin Cho Aye *et al.* (2024) [5] and Kaur *et al.* (2023) [6] have demonstrated that polymeric blends of chitosan with polyvinyl-based polymers such as PVP and PVA enhance drug release control, mechanical strength, swelling capacity, and overall biocompatibility. These synergistic interactions are especially beneficial in developing transdermal or wound-healing matrices where durability and sustained release are essential.

Bypassing the digestive system and hepatic first-pass metabolism, transdermal drug delivery systems (TDDS) offer a non-invasive, patient-compliant method of administration. Through unbroken skin, these devices carry the active medication straight into the systemic circulation, sustaining a constant therapeutic dose for a long time. TDDS improves therapeutic adherence by doing away with the necessity for frequent dosing. The advantages of sustained-release systems and nanotechnology can be combined into a single, convenient dosage form by incorporating HSLNs into a film-based transdermal matrix. The aim of the present study was to develop and evaluate a Herbal Solid Lipid Nanoparticle (HSLN) loaded transdermal film using chitosan and polyvinyl alcohol (PVA) as a polymeric base, for the effective and sustained delivery of Boswellic acid in a carrageenan-induced arthritis model in rats. The formulation was designed to overcome the limitations of oral phytomedicine delivery, such as poor bioavailability and gastrointestinal degradation, while enhancing skin permeation, stability and anti-inflammatory efficacy.

MATERIALS AND METHODS

Materials

Stearic acid, Chitosan, Glycerin, Acetic acid and Ethyl acetate were obtained from Sisco Research Laboratories Pvt. Ltd., Maharashtra. Polysorbate 80 was purchased from Alpha Chemika, Mumbai. Polyvinyl alcohol was obtained from HI Media Laboratories Pvt. Ltd., Mumbai. Toluene was obtained from Aventor Performance Materials India Limited. Maharashtra. Ethanol was purchased from Changshu Hongsheng Fine Chemical Co., Ltd., China. A lipid-based herbal extract of *Boswellia serrata* (in sesame oil base) was procured from

the RamaVarier Ayurveda foundation, Vilachery, Madurai and used as the active ingredient in the formulation. The presence of boswellic acids was confirmed by UV spectroscopic analysis using a standard boswellic acid reference. Wistar albino rats were used for animal testing. The chitosan used had a molecular weight of 15-300kDa and a degree of deacetylation >85%, as specified by the supplier.

Methods

Preparation of herbal solid lipid nanoparticle (HSLN)

Herbal solid lipid nanoparticles were developed using the hot homogenization technique. For optimal homogeneity, stearic acid was melted and mixed with *Boswellia serrata* lipid-based extract. The ratio of lipids to drug was kept at 8:1. Polysorbate 80 was dissolved in distilled water to form an aqueous phase. The melted lipid-drug phase (70 °C) was added to the surfactant phase maintained at the same temperature, followed by homogenization at 15,000 rpm for 15 min using a high-speed homogeniser. Solid lipid nanoparticles were formed when the resultant hot nanoemulsion cooled to room temperature. The cooling was achieved by gradual stirring at ambient conditions, avoiding thermal shock, to ensure controlled crystallization. For additional characterization and integration into the transdermal film matrix, the HSLN dispersion was kept at ambient temperature [7].

Formulation of herbal SLN-loaded transdermal film

A combination of Polyvinyl alcohol (PVA) and chitosan was used to generate a polymeric matrix for the development of transdermal films. Acetic acid was used to dissolve the chitosan solution, and distilled water was used to dissolve the PVA solution. To ensure uniformity, glycerine and the *Boswellia*-loaded lipid extract were added to the polymer blend. The term "herbal oil" in this context refers to the *Boswellia serrata* extract incorporated within the HSLN system; no separate oil was added at the film stage. To aid in solvent evaporation and film formation, the mixture was subsequently dried for five hours in a hot air oven. After that, the clear film was kept in a desiccator for additional analysis. Table 1 provides specifics on the film formulations [8]. Although SEM analysis was not performed on the film formulations (F1–F3), uniformity was confirmed by drug content analysis, swelling index, and *in vitro* release profiles. Future studies will include cross-sectional SEM imaging to directly visualize nanoparticle distribution within the films.

Table 1: Formulation of herbal film

Formulation	PVA: Chitosan (by weight)	Herbal Oil/HSLN(ml)/	Observation
HSLN F1	5: 2	2	Thin, flexible film formed, content is dispersed uniformly
HSLN F2	4: 2	1	Thin, flexible film formed, content is dispersed uniformly
HSLN F3	5: 2	1	Thin, flexible film formed, content is dispersed uniformly

UV-visible spectrophotometric analysis

Using UV-Visible spectrophotometric analysis, the study verified the existence and optical characteristics of herbal solid lipid nanoparticles (HSLNs). The HSLN was dissolved in methanol, vortexed and filtered as part of the procedure. The encapsulation of Boswellic acid was confirmed by the spectral scan, which showed a significant absorption peak between 200-800 nm. The analysis established a baseline reference for additional stability and quantitative research by validating the encapsulation method.

Particle size and zeta potential analysis of HSLN

Employing a Zetasizer 3000 HAS, the study examined the zeta potential and particle size distribution of herbal solid lipid nanoparticles (HSLNs). The purpose of the analysis was to ascertain the formulation's colloidal stability and homogeneity, which are essential for efficient drug delivery and extended shelf life. Dynamic light scattering was used to assess the hydrodynamic diameter after the sample was prepared by dilution with Milli-Q water. Electrophoretic light scattering was used to measure the zeta potential [9].

Scanning electron microscopy (SEM) analysis of HSLN

SEM was used in the study to analyze the size distribution and surface appearance of herbal solid lipid nanoparticles (HSLNs). It was discovered that the HSLNs primarily had smooth, well-defined surfaces and were spherical to slightly oval. The hydrodynamic sizes determined by dynamic light scattering were confirmed by the bulk of particles falling inside the nanoscale range. Boswellic acid was shown to be uniformly embedded in the lipid matrix rather than crystallising on the particle surface, which is essential for stable and reliable drug release [10].

Fourier-transform infrared (FTIR) spectroscopy

Potential chemical interactions between the lipid-polymeric matrix excipients and active phytoconstituent in the herbal solid lipid nanoparticle (HSLN) film were examined using Fourier-transform infrared (FTIR) spectroscopy. The final HSLN-Loaded film, excipients and synthesized HSLNs were dried and ground into fine particles to develop the samples. Between 400 and 4000 cm⁻¹, FTIR spectra were obtained, demonstrating hydrogen bonding interactions between the drug and the lipid matrix. The HSLN film

also displayed different peak positions and new absorption bands, indicating probable intermolecular interactions between the lipid nanoparticles and polymeric film-forming ingredients [11, 12].

In vitro drug release using the franz diffusion cell method

The Franz diffusion cell apparatus was used to assess the *in vitro* drug release of a film coated with herbal solid lipid nanoparticles. After being soaked in sodium hydroxide, the film was put between the donor and receptor compartments on a cellulose acetate membrane. Phosphate buffer (pH 7.4) solution was added to the receptor compartment, which was kept at 37 °C and constantly stirred. A UV-Visible spectrophotometer was used to absorb the sample at 234 nm. The formulation's sustained release characteristic was shown by calculating the cumulative percentage of drug release. Based on the drug release, the optimized formulation will be selected [13].

Release kinetics using a mathematical model

The release kinetics of the optimized HSLN film were analyzed by fitting the *in vitro* drug release data into various mathematical models, including zero-order, first-order, Higuchi, and Korsmeyer-Peppas models. The zero-order model was evaluated by plotting cumulative drug release versus time to determine if the release occurred at a constant rate. The first-order model was assessed by plotting the logarithm of the cumulative drug remaining versus time, indicating whether the release was concentration-dependent. The Higuchi model was applied by plotting cumulative drug release against the square root of time to assess diffusion-controlled release. The Korsmeyer-Peppas model was used to determine the mechanism of drug release by plotting the logarithm of cumulative drug release versus the logarithm of time, where the diffusion exponent (n) was analyzed to classify the release mechanism as Fickian diffusion, non-Fickian transport, or case-II transport. The correlation coefficient (R²) of each model was calculated to identify the best-fit kinetics, providing insights into the drug release mechanism from the HSLN film [14].

DPPH radical scavenging assay

The DPPH radical scavenging technique was used to evaluate the antioxidant activity of an optimized HSLN film. Methanol was used to dissolve the film, and various concentrations (100,200,400,800,1000 µg/ml) were examined. A 0.1 mmol DPPH solution was added to each tube, and ascorbic acid was employed as a reference antioxidant. In order to determine the % suppression of DPPH radical, the absorbance was measured at 517 nm using a UV-Visible spectrophotometer. The percentage inhibition of DPPH radicals was calculated using the following formula:

$$\text{Scavenging activity (\%)} = \left(\frac{A_0 - A_s}{A_0} \right) \times 100$$

Where A₀ is the absorbance of the control and A_s is the absorbance of the sample. The scavenging activity was determined at different concentrations to quantify the antioxidant potential. All measurements were performed in triplicate for accuracy [15].

Nitric oxide scavenging assay

The Griess reagent method, which measures nitrite generation as a sign of nitric oxide production, was used to assess the optimized HSLN nitric oxide scavenging activity. The HSLN film was dissolved in methanol to develop the test solutions at different concentrations, and sodium nitroprusside was employed as a nitric oxide donor. To produce nitric oxide, the mixture was incubated for 150 min at 25 °C in the presence of light. The reaction mixture was moved to a fresh tube and combined with the Griess reagent following incubation. After 10 min of dark incubation at room temperature, the pink solution was tested for absorbance at 546 nm. The formulation was used to determine the nitric oxide scavenging activity.

$$\text{Scavenging activity (\%)} = \left(\frac{A_0 - A_s}{A_0} \right) \times 100$$

Where A₀ is the absorbance of the control and A_s is the absorbance of the sample. All the values were recorded as mean±SD from three replicates.

In vitro anti-inflammatory assay of the optimized HSLN film

Protein denaturation inhibition

The HSLN film's ability to prevent heat-induced protein denaturation was assessed using the protein denaturation assay. A 0.2% W/V solution of bovine serum albumin (BSA), a standard protein, was made in phosphate-buffered saline. HSLN film test samples were made with a concentration between 10 and 100µg/ml. After 20 min of incubation at room temperature, the combinations were heated for 20 min at 57 °C in a water bath. At 660 nm, the absorbance was measured with a UV-visible spectrophotometer. Diclofenac sodium served as the positive standard, and a control was made using BSA and solvent devoid of the sample. The formula was used to determine the % inhibition of protein denaturation [16].

$$\text{Inhibition (\%)} = \left(\frac{A_0 - A_s}{A_0} \right) \times 100$$

Where A₀ is the absorbance of the control and as is the absorbance of the test samples

Protease inhibition assay

The enzyme-substrate system of trypsin and casein was used to evaluate the protease-inhibitory activity of the HSLN film. The test sample was pre-incubated with trypsin for 5 min after a trypsin solution was made in Tris-HCl buffer. After adding casein, 70% perchloric acid was used to stop the process. At 210 nm, the supernatant's absorbance was measured [16].

$$\text{Inhibition (\%)} = \left(\frac{A_0 - A_s}{A_0} \right) \times 100$$

Where A₀ is the absorbance of the control and as is the absorbance of the test samples

Lipoxygenase inhibition assay

The study used soybean lipoxygenase and Linoleic acid as substrates to assess the inhibition of lipoxygenase, an enzyme essential to leukotriene production. Test samples were preincubated with an enzyme solution for 5 min after it was made in borate buffer. Over six minutes, the absorbance increase was tracked, and the % inhibition of LOX activity was noted and the reference standard was diclofenac sodium. Every experiment was carried out in triplicate, and the mean±SD was used to express the results [16].

In vitro cell line studies for the optimized HSLN film [17]

MTT assay on RAW 264.7 cells

The MTT assay was used to evaluate the herbal solid lipid nanoparticles (HSLN) film on RAW 264.7 murine macrophage cells. In comparison to untreated LPS-stimulated control and standard diclofenac sodium (50 and 100µg/ml), the cells were treated with different concentrations of HSLN film (25,50,100 and 200 µg/ml). Untreated cells and LPS-only treated cells were used as negative and positive inflammation controls, respectively. Diclofenac sodium (50 and 100 µg/ml) served as the standard.

Effect of nitric oxide production in Raw 264.7

By evaluating the production of nitric oxide in Raw 264.7 macrophages activated by lipopolysaccharide (LPS), the anti-inflammatory effectiveness of HSLN was assessed. The test samples' anti-inflammatory activity is demonstrated by their capacity to suppress no generation, The Griess reagent test was used to measure the amount of nitrate in the culture supernatant using the untreated LPS-stimulated group as the control.

In vivo skin irritation test for the optimized HSLN film

The primary skin irritation test was conducted using wistar rats to assess the dermal safety of the optimized HSLN film formulation. Before the experiment, the rats were acclimatised, and their dorsal fur was shaved 24 h before film application. The formulation was applied onto the skin of test animals and covered with gauze. Observations for erythema and edema were made at 24, 48, and 72 h post-application. The severity of reactions was graded according

to the draize scoring system. The primary irritation index (PII) was calculated to classify the irritancy level of the formulation. Histological examination using H and E staining was not performed in this study due to technical constraints; however, this is acknowledged as a limitation and planned for future studies.

Determination of carrageenan-induced paw edema

The carrageenan-induced rat paw edema model was used to evaluate the anti-inflammatory activity of the boswellia-loaded HSLN film. Inflammation was induced by injection of 0.1 ml of 1% carrageenan solution into the subplantar region of the left hind paw. Animals were divided into control, standard and treatment groups (n=6). Paw volume was measured at 0, 1, 2, 4, and 8 h using a plethysmometer and the percentage inhibition of edema was calculated in comparison to the control. All procedures involving animals were approved by the institutional animal ethics committee (IAEC) with approved number (IAEC No-AU/CAF/PT/2020/002) and conducted in accordance with CPCSEA guidelines [18]. The animals were procured from a CPCSEA-approved registered vendor.

$$\% \text{ inhibition of edema} = \left(1 - \frac{V_t}{V_c}\right) \times 100$$

Where V_t represents the paw volume in the test group, and V_c represents the paw volume in the control group. The data were statistically analyzed, and comparisons were made between groups to determine the anti-inflammatory potential of the HSLN film. The study followed ethical guidelines and was approved by the Institutional Animal Ethics Committee.

Statistical analysis

All experimental data are expressed as mean \pm standard deviation (SD). *In vitro* studies were conducted in triplicate (n = 3), and *in vivo* tests used six animals per group (n = 6). One-way ANOVA followed by Tukey's post hoc test was used for multiple comparisons, with $p < 0.05$ considered statistically significant. GraphPad Prism version 9.0 was used for statistical analysis and plotting.

RESULTS AND DISCUSSION

Particle size and zeta potential

Herbal solid Lipid Nanoparticles (HSLNs) nanoscale size that can enhance medication delivery by improving cellular absorption and bioavailability. Particles smaller than 200 nm have been shown in studies to improve bioavailability. The average particle size of the HSLN formulation was found to be 101.9 nm, with a polydispersity index (PDI) of 0.410, indicating moderate size uniformity (fig. 1). According to Malvern Instruments guidelines, a PDI value below 0.5 indicates an acceptable monodispersity for topical nanocarrier systems. This finding is consistent with Zhou *et al.* (2022) research, which shows a homogeneous particle size distribution [19]. The zeta potential of -29.9 mV (fig. 2), significant, suggesting good colloidal stability. Formulations with zeta potentials beyond ± 25 mV are generally considered physically stable, due to sufficient electrostatic repulsion. This supports the long-term dispersion stability of the developed formulation. Samee *et al.* (2023) also demonstrated that sulconazole-loaded HSLNs had zeta potential values ranging from -16.40 to -28.52 mV [20]. Thus, the current formulation possesses promising physicochemical attributes suitable for transdermal drug delivery.

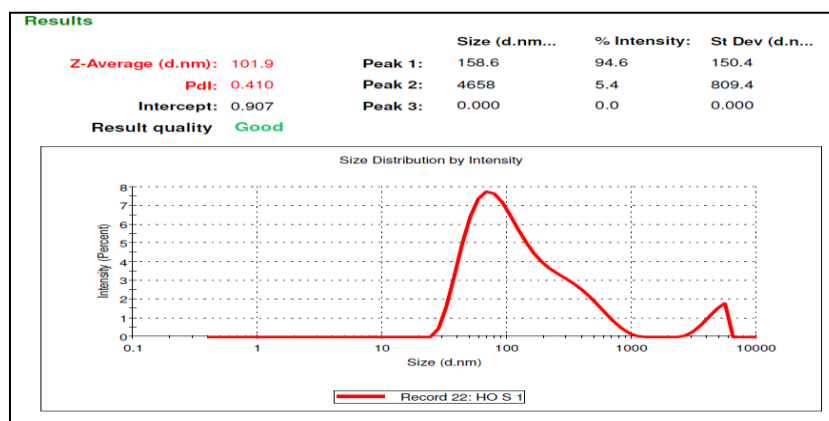


Fig. 1: Particle size distribution of Boswellia-loaded HSLNs as determined by dynamic light scattering (DLS). The Z-average diameter was 101.9 nm with a polydispersity index (PDI) of 0.410

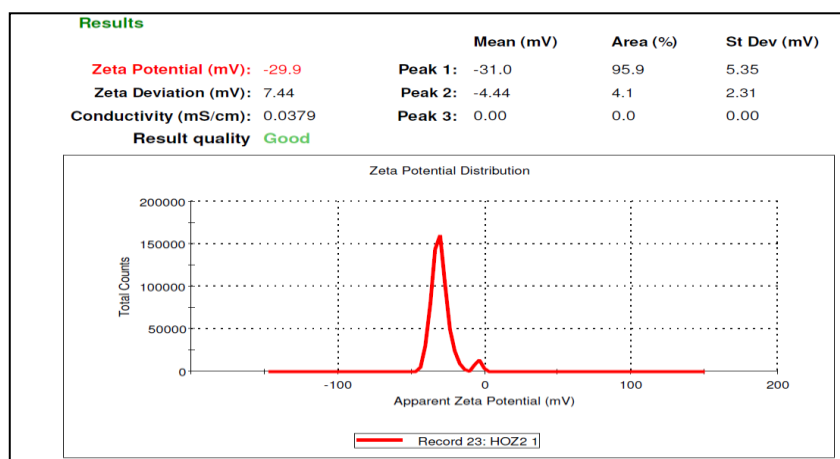


Fig. 2: Zeta potential distribution of Boswellia-loaded HSLNs showing a mean zeta potential of -29.9 mV

UV-visible spectrophotometric analysis

The HSLN formulation's UV-Visible spectroscopy analysis revealed a strong absorption peak at 234 nm (fig. 3), indicating that boswellic acid was well encapsulated inside the lipid matrix. This supported the formulation's integrity for additional therapeutic evaluation by showing good solubility and stable dispersion.

SEM analysis

Scanning electron microscopy (SEM) was used in the study to examine the produced nanoparticles' surface appearance and particle size distribution (fig. 4). The findings demonstrated

homogeneous, evenly distributed nanoparticles with a large surface area and the potential for improved drug loading. The range of particle sizes, which was 31.3 nm to 156.9 nm, demonstrated how well the formulation approach worked to achieve nanoscale dimensions. Quantitative particle size annotations were added directly to the SEM micrographs at 80,000x Magnification, confirming size uniformity and narrow distribution within the nanoscale range. SEM images include clear scale bars at all magnifications to support accurate morphological interpretation. The formulation's stability and homogeneity are supported by the SEM analysis, which gives it promise for use in therapeutic settings.

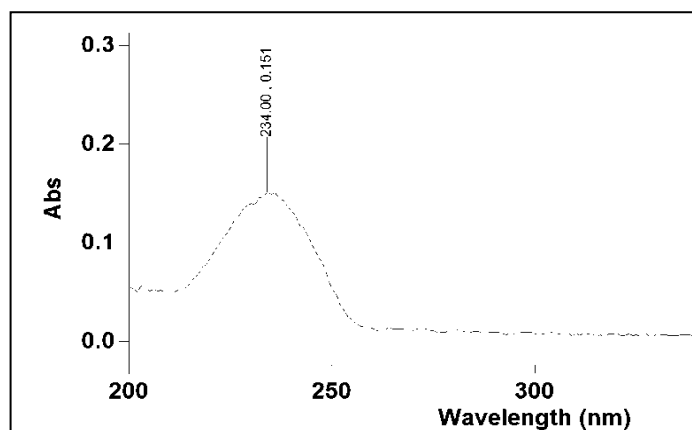


Fig. 3: UV-visible absorption spectrum of herbal solid lipid nanoparticles (HSLN) formulation, showing a characteristic absorption peak at 234 nm with an absorbance of 0.151, indicating successful encapsulation of the bioactive compound within the lipid matrix

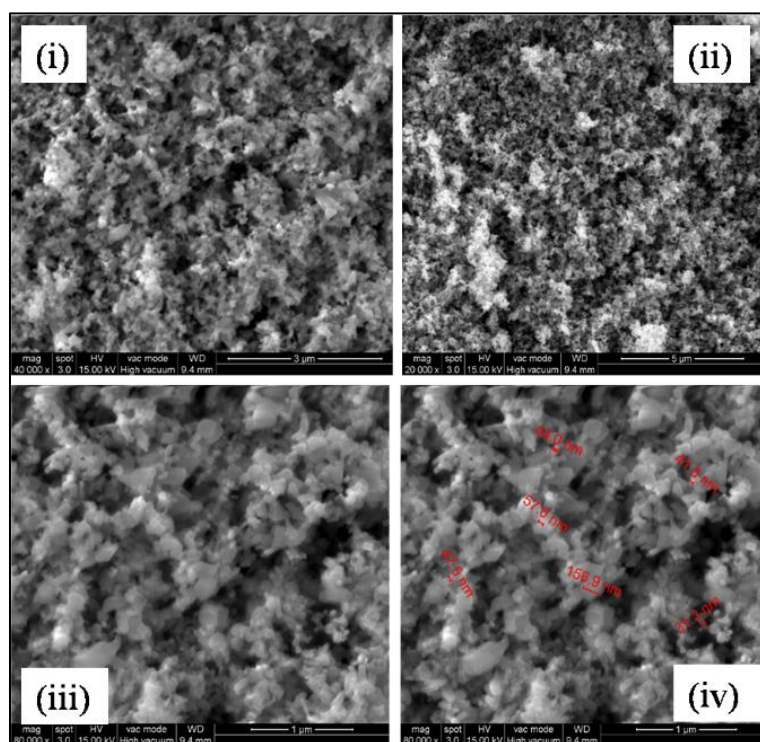


Fig. 4: Scanning electron microscope photographs of HSLN at different magnifications (i) 20,000X, (ii) 40,000X, (iii) 80,000X and (iv) 80,000X with scale

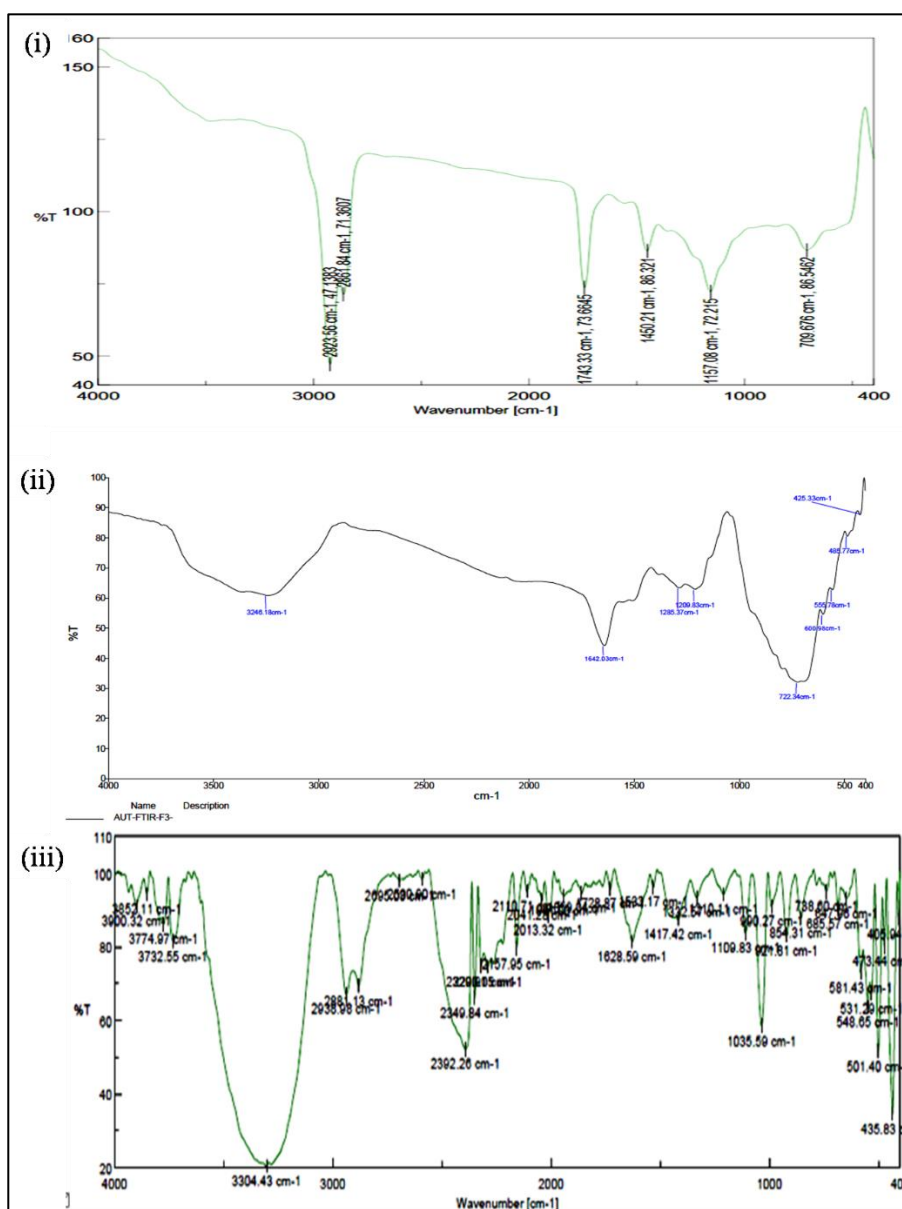
FTIR study

The FTIR spectra analysis of the herbal oil, HSLN, and HSLN-loaded film revealed significant interactions indicative of successful

encapsulation and incorporation (fig. 5). The herbal oil exhibited characteristic peaks at 2920.65 cm^{-1} and 2850.68 cm^{-1} , corresponding to $-\text{CH}_2$ and $-\text{CH}_3$ stretching vibrations, and a strong peak at 1742.33 cm^{-1} , indicative of $\text{C}=\text{O}$ stretching in lipid esters.

Upon encapsulation into HSLNs, a noticeable shift and slight broadening of the C=O peak were observed, suggesting hydrogen bonding interactions between the lipid phase and the drug molecules. Additional shifts in peak positions, particularly around 3306.18 cm^{-1} , suggested hydrogen bonding between the herbal oil and the lipid matrix. This observation aligns with findings from a study on Neem oil-loaded HSLNs, which reported similar spectral shifts due to interactions between bioactive compounds and lipid carriers [21]. In addition, the HSLNs exhibited a peak around 1464.52 cm^{-1} corresponding to C-H bending vibrations, and a peak near 1235.76 cm^{-1} , which can be attributed to C-O stretching of ester or alcohol groups present in the lipid and bioactive components. A small but consistent band between $1540\text{--}1550\text{ cm}^{-1}$ may be attributed to amide II vibrations from chitosan, while a broader band near $1650\text{--}1660\text{ cm}^{-1}$ corresponds to amide I stretching, indicating possible hydrogen bonding between chitosan's amino

groups and boswellic acids. Peaks in the $1020\text{--}1040\text{ cm}^{-1}$ range correspond to C-N stretching from chitosan, further confirming polymer-drug compatibility. The presence of multiple bands below 900 cm^{-1} in the fingerprint region is characteristic of the boswellic acid skeleton, confirming structural integrity post-formulation. In the HSLN-loaded film spectrum, further peak broadening at 3304.43 cm^{-1} and new peaks at 2340.84 cm^{-1} and 1628.50 cm^{-1} indicated molecular interactions between the lipid nanoparticles and the polymeric film matrix, ensuring uniform dispersion. These peak modifications suggest that chitosan's-NH₂ and PVA's-OH groups formed secondary interactions with the lipid carriers, stabilizing the HSLNs within the film. The presence of peaks at 1080.27 cm^{-1} (C-O-C stretching) and 840.91 cm^{-1} (C-H out of plane bending) further confirms the structural integration of polymers and lipid carriers. Such interactions may contribute to prolonged drug retention in the matrix and explain the sustained-release profile observed in the *in vitro* diffusion.



slightly higher PVA content in F2 improves hydrophilicity while chitosan contributes to bioadhesion and matrix integrity. These

findings align with previous studies, which support the observed properties of herbal-based films.

Table 2: Physicochemical properties of HSLN film

Formulation (HSLN film)	Weight variation (g)	Thickness (mm)	% Moisture content	Folding endurance (no's)	Moisture uptake (%)	Swelling index (%)	Surface pH	Drug content uniformity (%)
F1	0.0559±0.02	0.063±0.02	1.028±0.004	92	4.87±0.02	145.6±2.3	6.2±0.1	97.5±1.2
F2	0.0667±0.07	0.076±0.005	1.097±0.010	98	5.23±0.04	152.8±3.1	6.4±0.2	98.3±0.8
F3	0.0771±0.08	0.070±0.01	1.171±0.005	95	5.62±0.03	160.2±2.8	6.5±0.1	99.1±1.0

Value are represented as mean±SD, n=6

In vitro drug release and its kinetics from the herbal film

The study found a time-dependent drug release pattern (fig. 6) for all formulations (F1, F2, and F3). F2 showed a higher release than F1 and F3, possibly due to surface-associated drug dissolution. By 60 min, F3's release was slightly higher than F1 but lower than F2, indicating formulation-dependent release characteristics. F3 showed the highest release beyond 90 min, suggesting enhanced solubility and permeability. F1 followed a progressive release, reaching 98.38% at 360 min, while F2 exhibited a slower, more

controlled release. The differences in drug release profiles among formulations highlight the role of excipient composition, polymer matrix, and particle size in modulating drug release kinetics. F2 is regarded as the optimal formulation based on the drug release, and additional analysis was conducted using F2. The Biphasic drug release observed in F2 can be attributed to an initial burst from the surface-associated drug, followed by controlled diffusion through the polymeric matrix. This sustained phase likely arises due to hydrogen-bonded entrapment within the lipid-polymer interface.

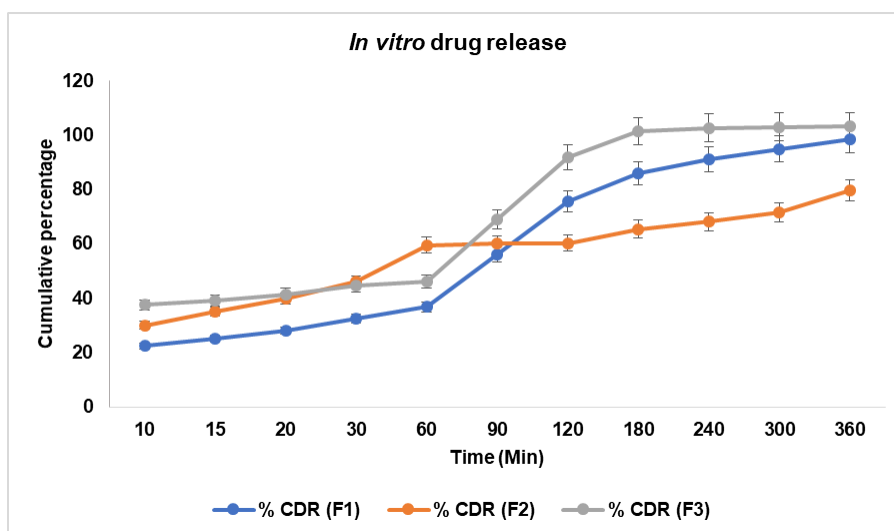


Fig. 6: Cumulative percentage of drug released from the herbal films

Release kinetics

The Release pattern of the F2 film is biphasic (table 3), with a moderate release during the 1st hour and continuous release for the next six hours. The logarithmic decay of the remaining drug in the matrix and drug release appear to be more strongly correlated according to the first-order kinetics model. With a higher R² value of 0.920, the Higuchi model, which characterizes drug release as a

diffusion process, indicates that the F2 film primarily operates as a diffusion-controlled delivery system. The nearly perfect connection offered by the Korsmeyer-Peppas model points to an abnormal or non-Fickian release profile that involves both diffusion and mechanisms of polymer relaxation or erosion. Because a drug delivery method that uses non-Fickian kinetics offers regulated sustained release without a significant initial burst, these findings have practical relevance for transdermal applications.

Table 3: Correlation coefficients (R²) of various kinetic models applied to the drug release profile of HSLN transdermal film formulation F2, indicating the best fit with the Korsmeyer-Peppas model

Model	Zero order	First order	Higuchi	Korsmeyer-peppas
R ²	0.807	0.909	0.920	0.956

DPPH assay

The DPPH free radical scavenging assay was used to evaluate the antioxidant capability of the HSLN film (fig. 7). Ascorbic acid demonstrated a greater percentage of inhibition at every dose point, and the film demonstrated a concentration-dependent increase in

DPPH scavenging activity. At 100µg/ml, the HSLN film showed 38.5% inhibition, whereas ascorbic acid showed 65.4%. Given its intricate encapsulated matrix, which most likely contained boswellic acids and other herbal bioactive ingredients, the HSLN film's performance was excellent. At higher concentrations, the performance disparity was reduced, with HSLN attaining about 90% inhibition at 1000 µg/ml.

The efficacy of the HSLN film at greater dosages raises the possibility that it could be used as an antioxidant, particularly for extended topical treatment. The result of the DPPH experiment validates the HSLN antioxidant claim and its function in treating illnesses linked to oxidative stress. Since oxidative stress and inflammation are closely related physiological processes, the discovered free radical neutralisation method may indirectly support the film's anti-inflammatory effectiveness. Notably, previous reports on free *Boswellia serrata* extracts (Satapathy *et al.*, 2023) [22] showed

approximately 75.9 % inhibition in DPPH scavenging at the highest concentration tested, whereas our HSLN film achieved nearly 90 % inhibition under similar conditions. This highlights the clear advantage of encapsulation in enhancing antioxidant efficacy. The radical scavenging effectiveness of the HSLN film was significant, particularly at concentrations of greater than 800 µg/ml. According to these results, the film might be a useful antioxidant platform in the pharmaceutical application, especially in transdermal formulations intended to treat inflammation and wounds.

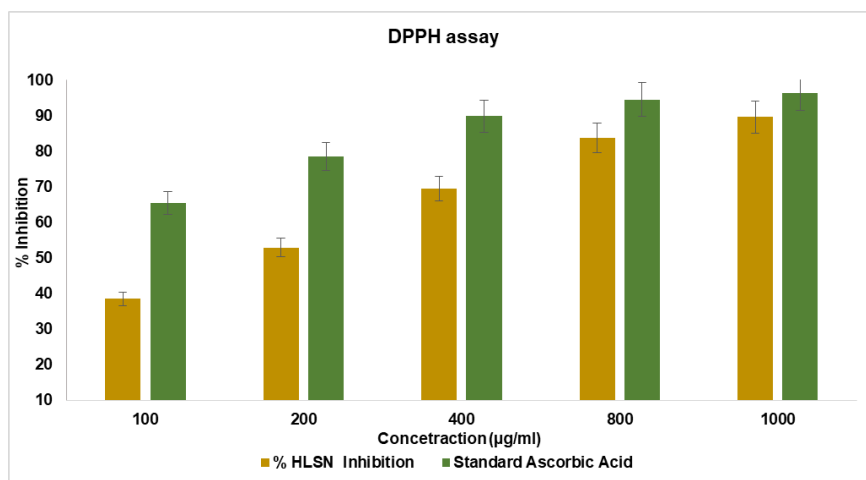


Fig. 7: DPPH radical scavenging activity of HSLN and ascorbic acid at 100–1000 µg/ml, expressed as % inhibition (mean±SD, n = 3) indicating a concentration-dependent increase in radical scavenging activity for both HSLN and standard

Nitric oxide

The anti-inflammatory and anti-oxidant properties of the HSLN film have been evaluated (Fig.8). In response to stress or infection, endothelial cells and macrophages release nitric oxide, a crucial inflammatory mediator. At 1000 µg/ml, the HSLN formulation demonstrated a dose-dependent increase in NO inhibition, approaching 86%. The presence of phytoconstituents, such as

boswellic acids, which control NO release and block inflammatory enzyme pathways, is the cause of this. The performance of the HSLN film is remarkable, particularly in light of its multifunctional matrix and complexity. The film demonstrated 85.9% inhibition at the maximum tested concentration, which is just less than the 94.8% observed with ascorbic acid. This implies that, especially in topical or transdermal application, the film may indirectly lessen the burden of inflammation in addition to providing antioxidant protection.

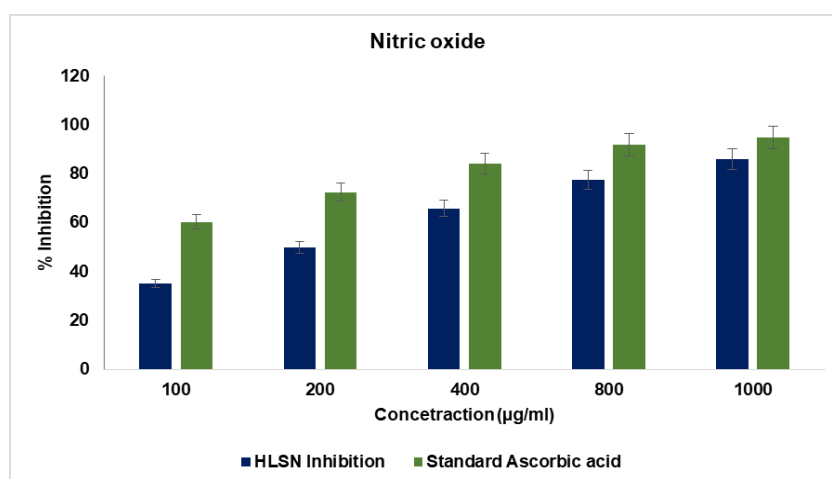


Fig. 8: % Inhibition of NO formation increased with concentration for both test and standard, showing strong dose-dependent trends, Value are shown as mean±SD (n = 3)

In vitro anti-inflammatory assay for the optimized HSLN film

Protein denaturation

Protein denaturation, a crucial process in autoimmune illnesses like rheumatoid arthritis, was strongly and concentration-dependently inhibited by the HSLN film. Because boswellic acids and other phytoconstituents block inflammatory signaling pathways, lower

leukocyte infiltration, and shield structural proteins from enzymatic destruction, the film can prevent protein denaturation. Particularly at higher doses (87.4% vs. 92.6% at 1000 µg/ml) (fig. 9), the HSLN film is just as effective as diclofenac sodium at preventing protein denaturation. The HSLN film has the benefit of being made from natural materials and may have fewer long-term adverse effects than the standard, although it is marginally less effective.

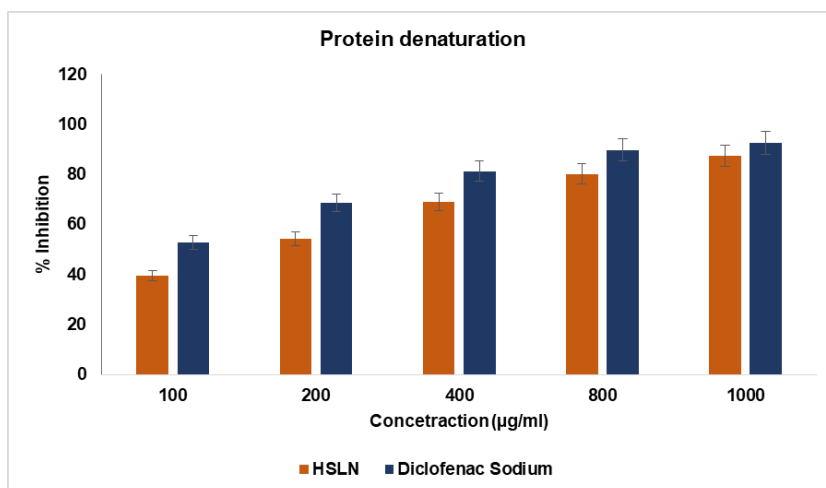


Fig. 9: Inhibition of heat-induced protein denaturation by HSLN and diclofenac sodium (100–1000 µg/ml), reported as % inhibition (mean±SD, n = 3)

Protease inhibition (%)

Trypsin was used as the model enzyme and casein as the substrate to assess the HSLN films' capacity to block proteases. Protease activity was dose-dependently inhibited in the film, increasing from 34% at 100 µg/ml to 51.6% at 200 µg/ml, 63.4% at 400 µg/ml, 76.2% at 800 µg/ml and 83.5% at 1000 µg/ml (fig. 10). At every concentration, diclofenac sodium, a common NSAID, showed greater inhibition. The lipid matrix and biopolymer constituents of the HSLN film, like polyvinyl

alcohol or chitosan, might be involved in the overall suppression of protease. The HSLN film's performance in the protein denaturation assay closely resembles its inhibitory trend, pointing to a more comprehensive anti-inflammatory mechanism that involves tissue-degrading enzyme suppression and extracellular protein stability. At higher doses, the film's capacity to achieve over 80% inhibition confirms its potential for further advancement in anti-inflammatory treatment. In summary, at higher dosages, the HSLN films' potent dose-dependent suppression of protease activity approached that of diclofenac sodium.

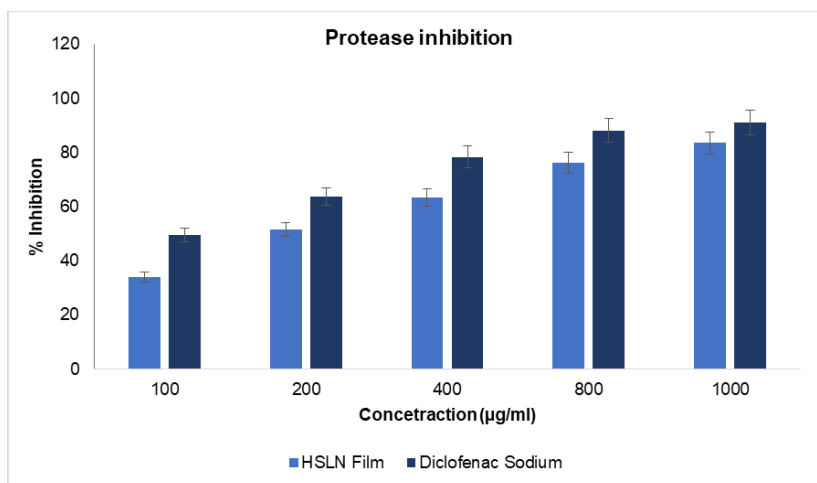


Fig. 10: Trypsin protease inhibition by HSLN and diclofenac sodium at different concentrations, shown as % inhibition (mean±SD, n = 3)

Lipoxygenase inhibition

An important mechanism in inflammation is the lipoxygenase (LOX) pathway, which transforms arachidonic acid to leukotrienes, which are connected to a number of dermatological disorders, arthritis and asthma. One well-known method of treating chronic inflammation is to inhibit LOX activity. Similar to synthetic NSAIDs, a study comparing the LOX inhibitory action of the HSLN film with diclofenac sodium revealed that the HSLN film significantly inhibited the LOX enzyme. At the investigated concentrations of 48.3%, 61.7%, 73.9%, 88.5% and 90.2%, respectively, the HSLN film showed progressive LOX inhibition. At each dose, diclofenac sodium demonstrated slightly greater inhibition, 55.4%, 70.1%, 83.9%, 91.8% and 94.5% (fig. 11). The primary active ingredients, boswellic acids, are well-established LOX inhibitors that target the 5-LOX variant that produces pro-inflammatory leukotrienes. The inhibitory trends of the HSLN film are consistent with those of earlier tests, indicating a steady anti-

inflammatory profile. The results are almost identical to those of diclofenac sodium, confirming the promise of this natural system as a substitute treatment for managing chronic inflammation. For transdermal application, the prolonged inhibition at greater concentrations shows great promise and provides a better safety profile. At the highest measured concentration, the HSLN film showed a strong and dose-responsive suppression of lipoxygenase activity.

MTT assay for the optimized HSLN film

The metabolic activity and visibility of RAW 26.7 murine macrophage cells were evaluated using the MTT test (fig. 12) after they were exposed to different concentrations of the HSLN film. To support the HSLN formulations' possible safety and effectiveness in biological systems, the major goal was to ascertain whether they maintained adequate cell viability across a range of concentrations. Although the HSLN formulation showed a dose-dependent reduction

in cell viability, all values were still higher than the commonly recognized-toxic 75% viability threshold. The lipid matrix and natural polymer in the formulation have an intrinsic biocompatibility, which may be the reason for the comparatively high vitality values for the HSLN-treated cells. Up to 200 $\mu\text{g/ml}$, the

HSLN film preserved satisfactory mitochondrial function, suggesting a wide safety margin for more biological research. The formulation's intended usage in transdermal distribution, where skin cells or immune cells like macrophages may come into extended contact with the formulation, increases the significance of this outcome.

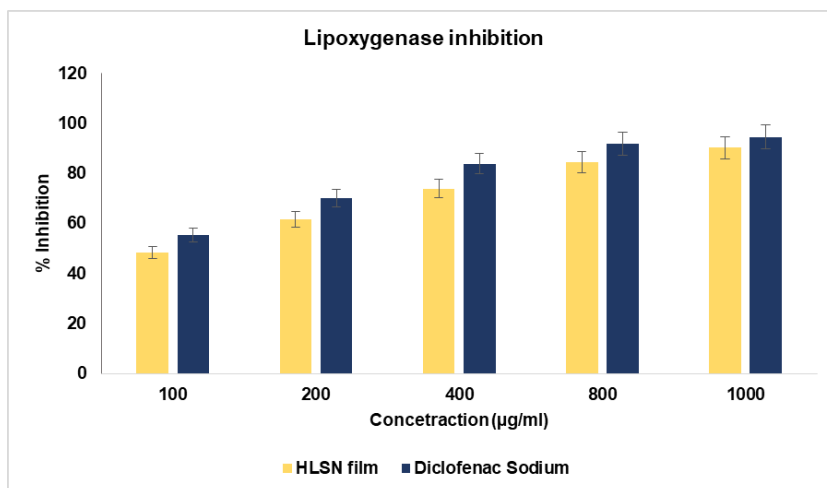


Fig. 11: Lipoxygenase inhibition by HSLN and diclofenac sodium (100–1000 $\mu\text{g/ml}$), expressed as % inhibition (mean \pm SD, n = 3)

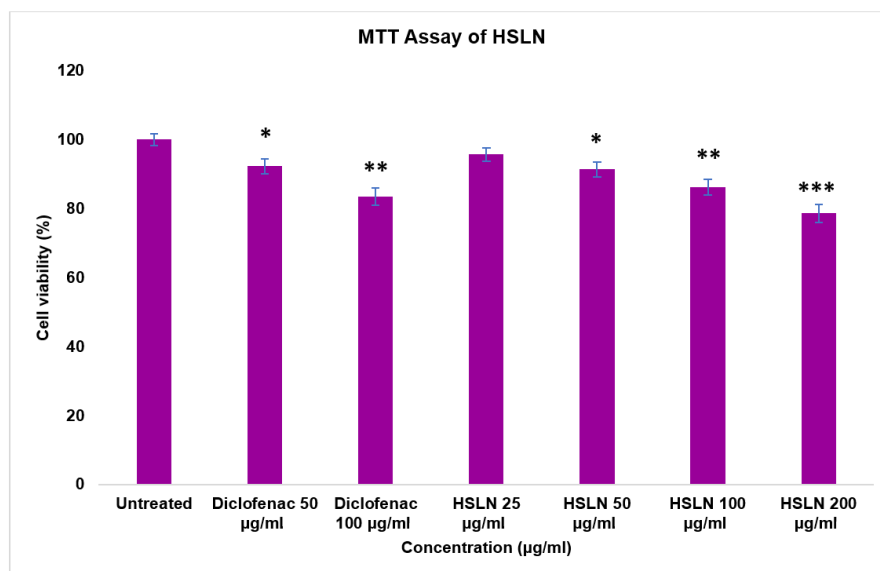


Fig. 12: Effect of HSLN on cell viability in RAW 264.7 macrophages assessed by MTT assay. Cells were treated with varying concentrations of HSLN (25–200 $\mu\text{g/ml}$) and standard diclofenac sodium (50 and 100 $\mu\text{g/ml}$) for 24 h. Untreated LPS-stimulated cells served as control. Data are presented as mean \pm SD (n=6). Statistical significance is indicated by asterisks: * p <0.05, ** p <0.01, *** p <0.001

Raw cell line for the optimized HSLN film

Using the griess assay, the study assessed the cytotoxicity of a formulation of HSLN in Raw 264.7 murine macrophage cells (fig. 13). Lipopolysaccharide (LPS) was used to stimulate the cells in order to trigger the synthesis of NO through inducing nitric oxide synthase (iNOS). The inflammatory response was successfully activated, as seen by the increased NO levels in the untreated group. Following that, the cells were exposed to progressively higher doses of either the HSLN formulation or diclofenac sodium. The findings demonstrated that both the diclofenac and HSLN-treated groups reduced NO generation in a dose-dependent manner. In comparison to the untreated control, diclofenac sodium dramatically decreased nitrate levels to 25.6 ± 1.2 μM at 50 $\mu\text{g/ml}$ and 18.3 ± 1.4 μM at 100 $\mu\text{g/ml}$. Notably, the similar effectiveness of diclofenac at 100 $\mu\text{g/ml}$ and HSLN at 200 $\mu\text{g/ml}$. The finding demonstrated that both groups'

NO production decreased in a dose-dependent manner. The inflammatory response in macrophages was found to be effectively modulated by HSLN, indicating that phytoconstituents incorporated in the lipid matrix may scavenge reactive nitrogen species or inhibit the iNOS pathway.

Skin irritation test for the optimized HSLN film

The skin irritation study results, as shown in fig. 14, demonstrate the dermal response of the control, standard, and test formulation groups at 0 h (i, iii, v) and after 72 h (ii, iv, vi). The control group (i, ii) exhibited no significant irritation, maintaining normal skin appearance. The standard group (iii, iv) showed mild to moderate erythema and edema, indicating some level of irritation. In contrast, the test formulation (v, vi) displayed no visible signs of skin irritation, confirming its biocompatibility and suitability for transdermal

application. The absence of erythema and edema in the test group suggests that the formulation is well-tolerated and safe for topical use. These findings support its potential for further dermatological

applications. Histological H and E staining was not performed due to technical constraints, but will be included in future work to further validate dermal safety at the microscopic level.

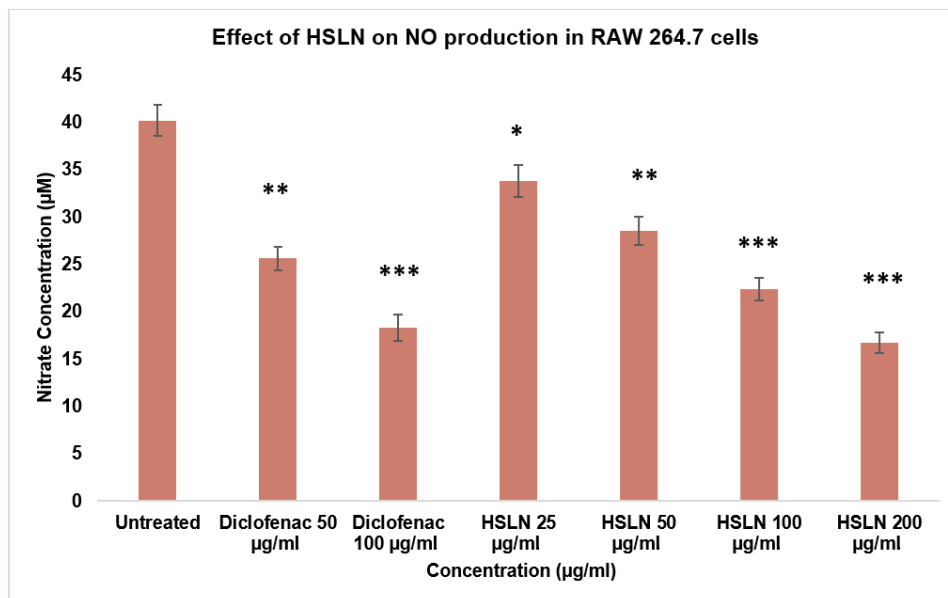


Fig. 13: Effect of HSLN on nitric oxide production in LPS-stimulated RAW 264.7 macrophages, Cells were treated with various concentrations of HSLN and standard diclofenac sodium for 24 h. Nitrite accumulation in the culture medium was quantified using the Griess assay. Data are expressed as mean±SD (n=6). Statistical significance is indicated by asterisks: * $p<0.05$, ** $p<0.01$, *** $p<0.001$

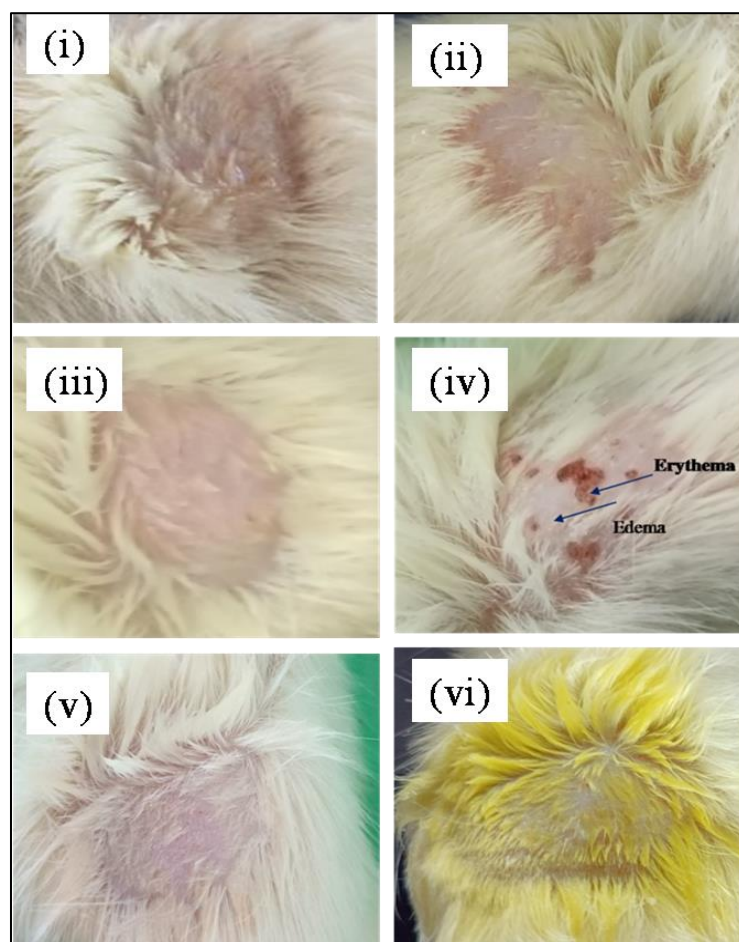


Fig. 14: Photographs of skin irritation study at 0h (i, iii, v) and 72h (ii, iv, vi for control, standard and formulation, respectively

Determination of carrageenan-induced paw edema for the optimized HSLN film

The anti-inflammatory potential of the test formulation was assessed using the paw edema method, and the results are presented in table 4. The control group exhibited a steady increase in paw volume over time, indicating persistent inflammation. In contrast, the standard drug-treated group showed a significant reduction in paw volume from 1 hour onwards, with a marked decrease to 0.4 ml at 8 h, demonstrating its potent anti-inflammatory effect. The formulation-treated group also

exhibited a progressive reduction in paw volume, mirroring the standard treatment, with a final value of 0.4 ml at 8 h. These findings suggest that the test formulation effectively reduces inflammation and may have comparable anti-inflammatory efficacy to the standard drug. The observed reduction in paw volume indicates the formulation's potential to inhibit edema formation, likely due to its bioactive constituents. The trends observed in enzyme inhibition assays and *in vivo* paw edema reduction were consistent; however, a direct statistical correlation (e. g., Pearson's *r*) was not conducted in this study and is acknowledged as a limitation.

Table 4: Paw volume of control, standard and sample treated rats

Time treatment	Paw volume (in ml)				
	0 h	1 h	2 h	4 h	8 h
Control	0.6±0.09	0.6±0.09	0.8±0.08	0.8±0.04	0.8±0.09
Standard	0.7±0.08	0.7±0.04	0.6±0.04	0.5±0.04	0.4±0.04
Formulation	0.6±0.04	0.7±0.04	0.6±0.04	0.5±0.04	0.4±0.04

Value are represented as mean±SD, n=6.

DISCUSSION

To address the limited bioavailability of herbal extracts and the negative consequences of long-term NSAID usage in the treatment of rheumatoid arthritis (RA), the study developed a transdermal film loaded with herbal solid lipid nanoparticles (HSLN), the developed nano-herbal film, especially formulation F2, showed great promise as an anti-arthritis, controlled-release medication. When it came to homogeneity, mechanical strength, swelling index and drug content, F2 showed the best balanced profile. Similar enhancement in film strength and uniformity was reported by Qureshi *et al.* (2022) [23] who incorporated diclofenac-loaded SLNs into chitosan/PVA matrices for sustained anti-inflammatory delivery. Using the Korsmeyer-Peppas model, the electrostatic stability and sustained release behaviour of the film were verified. The biphasic release observed in F2 offers a dual therapeutic advantage, providing an initial burst for rapid symptom relief followed by a sustained phase for prolonged efficacy, which is particularly suitable for chronic inflammatory conditions like RA. This release profile is clinically significant, as it may improve patient compliance by reducing dosing frequency and minimizing gastrointestinal adverse effects commonly associated with long-term oral NSAID or Boswellia therapy. At higher doses, the film showed over 85% suppression in the DPPH and nitric oxide tests, indicating a robust radical scavenging capability. Comparable antioxidant activity was demonstrated in the work of Kumbhare *et al.* (2023) [24] who utilized curcumin SLNs in polymeric films, achieving similar DPPH inhibition percentages. At 1000µg/ml, the HSLN film showed similar results to diclofenac sodium, demonstrating competitive performance across biological assays. The observed *In vitro* enzyme inhibition closely aligned with the *In vivo* reduction in paw edema, suggesting good translational potential of the formulation from lab to preclinical settings. The formulation's safety at effective dosages was validated by cytocompatibility testing. The synergistic interaction between Boswellic acids and chitosan/PVA biopolymers may enhance skin retention, permeability and bioactivity, contributing to improved therapeutic outcomes. Such biopolymer-drug synergy is consistent with reports from Wang *et al.*, (2014) [25] who demonstrated enhanced skin permeability in transdermal chitosan-based film's pharmacodynamic significance was supported by the *in vivo* paw edema research, which demonstrated a considerable suppression of edema volume during 8 h. This result corroborates previous findings by Khayyat *et al.*, (2018) [26] who observed a similar time-dependent edema inhibition with boswellic acid-loaded liposomal gels in arthritic rats. As part of the characterisation, SEM analysis was conducted exclusively on the HSLNs prior to film incorporation to confirm nanoscale morphology; imaging of the final film matrix was not performed. While this limits morphological interpretation of the film itself, the uniform particle distribution and spherical shape observed in the HSLNs support their compatibility within the polymeric system. One limitation of this study is the lack of histological analysis in the skin irritation model; however, this is recognised and planned for future research. The study shows that

HSLN-loaded herbal films are an effective means to overcome phytochemicals' pharmacokinetic restrictions.

CONCLUSION

This study successfully developed and evaluated a nano-based herbal film for transdermal delivery, demonstrating significant anti-arthritis potential. The formulation exhibited stability, enhanced antioxidant activity, and sustained anti-inflammatory effects, comparable to standard treatment. The dual-function HSLN-chitosan/PVA matrix offered a biphasic release profile that supports both immediate and long-term symptom management. These findings support the application of nano-phytochemicals in arthritis management, offering a non-invasive and effective alternative to conventional therapies. Further investigations, including pharmacokinetics, long-term safety and histopathological skin analysis, will strengthen the clinical translation of this formulation.

FUNDING

Nil

ABBREVIATION

HSLN/SLNs – Herbal Solid Lipid Nanoparticles/Solid Lipid Nanoparticles, PVA – Polyvinyl Alcohol, SEM – Scanning Electron Microscopy, FTIR – Fourier-Transform Infrared Spectroscopy, PDI – Polydispersity Index, UV-Vis – Ultraviolet-Visible Spectroscopy, PBS – Phosphate-Buffered Saline, NO – Nitric Oxide, LPS – Lipopolysaccharide, BSA – Bovine Serum Albumin, LOX – Lipoxygenase, CIPE – Carrageenan-Induced Paw Edema, CPCSEA – Committee for the Purpose of Control and Supervision of Experiments on Animals, IAEC – Institutional Animal Ethics Committee, DMEM – Dulbecco's Modified Eagle Medium, MTT – 3-(4,5-Dimethylthiazol-2-yl)-2,5-Diphenyltetrazolium Bromide, SD – Standard Deviation, SEM – Scanning Electron Microscopy (SEM) analysis, RNS – Reactive Nitrogen Species, ROS – Reactive Oxygen Species, ANOVA – Analysis of Variance, R² – Correlation Coefficient, SI units – International System of Units.

AUTHORS CONTRIBUTIONS

Sonia K: Conceptualization, methodology design, supervision and critical review of the manuscript. R. Vijaya: investigation, data curation, *In vivo* pharmacological studies, and original draft preparation. Janani: formal analysis, characterization studies (FTIR, SEM, zeta potential) and validation. Kiruba Mohandoss: Project administration, *In vitro* experimental studies, statistical analysis, final manuscript editing and corresponding author responsibilities

CONFLICT OF INTERESTS

Declared none

REFERENCES

- GBD 2021 Rheumatoid Arthritis Collaborators. Global regional and national burden of rheumatoid arthritis, 1990-2020, and

- projections to 2050: a systematic analysis of the global burden of disease study 2021. *Lancet Rheumatol.* 2023;5(10):e594-610. doi: [10.1016/S2665-9913\(23\)00211-4](https://doi.org/10.1016/S2665-9913(23)00211-4), PMID 37795020.
2. Entezami P, Fox DA, Clapham PJ, Chung KC. Historical perspective on the etiology of rheumatoid arthritis. *Hand Clin.* 2011;27(1):1-10. doi: [10.1016/j.hcl.2010.09.006](https://doi.org/10.1016/j.hcl.2010.09.006), PMID 21176794.
 3. Jeong WY, Kwon M, Choi HE, Kim KS. Recent advances in transdermal drug delivery systems: a review. *Biomater Res.* 2021;25(1):24. doi: [10.1186/s40824-021-00226-6](https://doi.org/10.1186/s40824-021-00226-6), PMID 34321111.
 4. Bodke V, Tekade BW, Badekar R, Phalak SD, Kale M. Pulsatile drug delivery systems the novel approach. *Int J Pharm Pharm Sci.* 2024;16(2):1-11. doi: [10.22159/ijpps.2024v16i2.49960](https://doi.org/10.22159/ijpps.2024v16i2.49960).
 5. Aye KC, Rojanarata T, Ngawhirunpat T, Opanasopit P, Pornpitchanarong C, Patrojanasophon P. Development and characterization of curcumin nanosuspension embedded genipin crosslinked chitosan/polyvinylpyrrolidone hydrogel patch for effective wound healing. *Int J Biol Macromol.* 2024;274(1):133519. doi: [10.1016/j.ijbiomac.2024.133519](https://doi.org/10.1016/j.ijbiomac.2024.133519), PMID 38960235.
 6. Kaur M, Sharma A, Puri V, Aggarwal G, Maman P, Huanbutta K. Chitosan-based polymer blends for drug delivery systems. *Polymers (Basel).* 2023;15(9):2028. doi: [10.3390/polym15092028](https://doi.org/10.3390/polym15092028), PMID 37177176.
 7. Tridev SK, Gadela RV, Sruthi P, Priya V. Solid lipid nanoparticles: preparation techniques their characterization and an update on recent studies. *J App Pharm Sci.* 2020;10(6):126-41. doi: [10.7324/JAPS.2020.10617](https://doi.org/10.7324/JAPS.2020.10617).
 8. Priyanka P, Rekha SM, Devi AS. Review on formulation and evaluation of solid lipid nanoparticles for vaginal application. *Int J Pharm Pharm Sci.* 2022;14(1):1-8. doi: [10.22159/ijpps.2022v14i1.42595](https://doi.org/10.22159/ijpps.2022v14i1.42595).
 9. Senthilnathan RD, Hemalatha SH, V Gayathri G, Komala MK. Phyla nodiflora-derived silver nanoparticles in hydrogel formulations: a new approach to wound management. *Curr Trends Biotechnol Pharm.* 2024;18(3s):240-56. doi: [10.5530/ctbp.2024.3s.19](https://doi.org/10.5530/ctbp.2024.3s.19).
 10. Bhange AM, Pethe A, Hadke A. Design and development of phytosomal soft nanoparticles for liver targeting. *Int J Appl Pharm.* 2023;15(1):280-9. doi: [10.22159/ijap.2023v15i1.46303](https://doi.org/10.22159/ijap.2023v15i1.46303).
 11. Atiyah RS, Al Edresi S. Preparation and justification of nanofibres loaded mafenide using the electrospinning technique to control release. *Int J Appl Pharm.* 2024;16(2):224-30. doi: [10.22159/ijap.2024v16i2.49691](https://doi.org/10.22159/ijap.2024v16i2.49691).
 12. PH, Fatima S. Formulation and evaluation of oral fast dissolving films of naproxen sodium. *Int J Curr Pharm Res.* 2022;14(2):48-53. doi: [10.22159/ijcpr.2022v14i2.1953](https://doi.org/10.22159/ijcpr.2022v14i2.1953).
 13. SG, Chandrakala V, Srinivasan S. Development and evaluation of microspoon gel of an antifungal drug. *Int J Curr Pharm Sci.* 2023;15(1):30-41. doi: [10.22159/ijcpr.2023v15i1.2069](https://doi.org/10.22159/ijcpr.2023v15i1.2069).
 14. Kariznavi E, Hatami H, Abbaspour MR, Akhgari A, Garekani HA, Sadeghi F. *In vitro* evaluation of ethyl cellulose and polyvinyl pyrrolidone composite nanofibers for transdermal delivery of diclofenac diethylamine. *J Drug Deliv Sci Technol.* 2024;98:105897. doi: [10.1016/j.jddst.2024.105897](https://doi.org/10.1016/j.jddst.2024.105897).
 15. Jose D, Kumudha D. Synthesis, characterization and *in vitro* evaluation of vaterite microparticles. *Int J Appl Pharm.* 2024;16(5):252-7. doi: [10.22159/ijap.2024v16i5.51569](https://doi.org/10.22159/ijap.2024v16i5.51569).
 16. Gunathilake KD, Ranaweera KK, Rupasinghe HP. *In vitro* anti-inflammatory properties of selected green leafy vegetables. *Biomedicines.* 2018;6(4):107. doi: [10.3390/biomedicines6040107](https://doi.org/10.3390/biomedicines6040107), PMID 30463216.
 17. Mohandoss K, VV, SH. Cissus quadrangularis phytosomes bioactivity assessment: cytotoxic anti-inflammatory and antioxidant properties. *Asian J Biol Life Sci.* 2025;13(3):714-22. doi: [10.5530/ajbls.2024.13.87](https://doi.org/10.5530/ajbls.2024.13.87).
 18. Ben Khedir S, Mzid M, Bardaa S, Moalla D, Sahnoun Z, Rebai T. *In vivo* evaluation of the anti-inflammatory effect of *Pistacia lentiscus* fruit oil and its effects on oxidative stress. *Evid Based Complement Alternat Med.* 2016;2016:6108203. doi: [10.1155/2016/6108203](https://doi.org/10.1155/2016/6108203), PMID 28070202.
 19. Chen J, Li S, Zheng Q, Feng X, Tan W, Feng K. Preparation of solid lipid nanoparticles of cinnamaldehyde and determination of sustained release capacity. *Nanomaterials (Basel).* 2022;12(24):4460. doi: [10.3390/nano12244460](https://doi.org/10.3390/nano12244460), PMID 36558312.
 20. Samee A, Usman F, Wani TA, Farooq M, Shah HS, Javed I. Sulconazole-loaded solid lipid nanoparticles for enhanced antifungal activity: *in vitro* and *in vivo* approach. *Molecules.* 2023;28(22):7508. doi: [10.3390/molecules28227508](https://doi.org/10.3390/molecules28227508), PMID 38005230.
 21. Nemati S, Mohammad Rahimi H, Hesari Z, Sharifdini M, Jalilzadeh Aghdam N, Mirjalali H. Formulation of Neem oil-loaded solid lipid nanoparticles and evaluation of its anti-toxoplasma activity. *BMC Complement Med Ther.* 2022;22(1):122. doi: [10.1186/s12906-022-03607-z](https://doi.org/10.1186/s12906-022-03607-z), PMID 35509076.
 22. Purabiya P, Kaushik S, Satapathy A, Jain P. Pre-clinical evaluation for anti-inflammatory antioxidant and antibacterial potential of boswellia seratta. *Adv Pharmacol Clin Trials.* 2023;8(4):1-5. doi: [10.23880/apct-16000225](https://doi.org/10.23880/apct-16000225).
 23. Qureshi D, Pattanaik S, Mohanty B, Anis A, Kulikouskaya V, Hileuskaya K. Preparation of novel poly(vinyl alcohol)/chitosan lactate-based phase-separated composite films for UV-shielding and drug delivery applications. *Polym Bull.* 2022;79(5):3253-90. doi: [10.1007/s00289-021-03653-6](https://doi.org/10.1007/s00289-021-03653-6).
 24. Kumbhar S, Khairate R, Bhatia M, Choudhari P, Gaikwad V. Evaluation of curcumin-loaded chitosan nanoparticles for wound healing activity. *ADMET DMPK.* 2023;11(4):601-13. doi: [10.5599/admet.1897](https://doi.org/10.5599/admet.1897), PMID 37937244.
 25. Wang Q, Pan X, Wong HH, Wagner CA, Lahey LJ, Robinson WH. Oral and topical boswellic acid attenuates mouse osteoarthritis. *Osteoarthritis Cartil.* 2014;22(1):128-32. doi: [10.1016/j.joca.2013.10.012](https://doi.org/10.1016/j.joca.2013.10.012), PMID 24185109.
 26. Khayyal MT, El Hazek RM, El Sabbagh WA, Frank J, Behnam D, Abdel Tawab M. Micellar solubilisation enhances the anti-inflammatory activities of curcumin and boswellic acids in rats with adjuvant-induced arthritis. *Nutrition.* 2018;54:189-96. doi: [10.1016/j.nut.2018.03.055](https://doi.org/10.1016/j.nut.2018.03.055), PMID 30048884.